First publ. in: Journal of Physics / Condensed Matter, 12 (2000), 29, pp. 6575-6583

Colloidal gelation and non-ergodicity transitions

J Bergenholtz†, M Fuchs‡§ and Th Voigtmann‡

† Department of Physical Chemistry, Göteborg University, 412 96 Göteborg, Sweden
‡ Physik-Department, Technische Universität München, 85747 Garching, Germany

Received 1 February 2000

Abstract. Within the framework of the mode coupling theory (MCT) of structural relaxation, mechanisms and properties of non-ergodicity transitions in rather dilute suspensions of colloidal particles characterized by strong short-ranged attractions are studied. Results building on the virial expansion for particles with hard cores and interacting via an attractive square-well potential are presented, and their relevance to colloidal gelation is discussed.

(The figures in this article appear in colour in the electronic version; see `www.iop.org`)

1. Introduction

Colloidal gelation is a non-equilibrium transition observed in dispersions where short-ranged attractions exceeding a few k_BT are present [1–3]. It is accompanied by the formation of (denser) domains, which coarsen and finally freeze when the gel line is traversed [4, 5]. The resulting gels are amorphous solids exhibiting finite elastic moduli [6, 7]. Often, the gel structure is fractal [1, 5], typically at low densities [8], and often low-angle scattering peaks are observed, which are reminiscent of spinodal decomposition; in this case gelation manifests itself by an arrest of the time dependence of the peak position [1, 5, 8–10]. This explicit dependence on the time since quenching the suspension shows that colloidal gelation is a non-equilibrium phenomenon [3].

Colloidal gelation has been observed in colloid polymer mixtures [4, 5], in solutions of sterically stabilized colloidal particles if the solvent quality is decreased [6, 7, 9], in emulsions [2], in solutions of charge-stabilized particles upon changes of the salt content [1], and in protein solutions [11]. In the last case, it prevents protein crystallization and thus is an important obstacle to the collection of protein structure information [12–14].

Previous theoretical explanations of colloidal gelation have focused on the possibility of a dynamic percolation within a gas–liquid phase coexistence region which is metastable with respect to gas–solid coexistence [3]. The gel is assumed to form when the largest cluster spans the sample and the small-angle scattering peak consequently arrests. Long-ranged density fluctuations could arise from quenching below metastable [15] spinodal lines as argued in references [6, 9, 10, 16]. Fine-tuning of the attraction strength allows for the observation of all aspects of spinodal decomposition in this systems without arrest and gelation [5, 8]. At low densities irreversible cluster–cluster aggregation provides a mechanism explaining the observed small-wave-vector structures [17]. A review of experiments and theoretical approaches up to 1997 has been given by Poon and Haw [3].

§ Author to whom any correspondence should be addressed.

Recently an alternative explanation for the arrest of the dynamics at colloidal gel transitions has been put forward [18,19]. Non-ergodicity transitions triggered by the local dynamics were suggested. Solutions of equations of the mode coupling theory (MCT) for structural relaxation [20,21] were studied which exhibit a localization transition explaining a number of properties of colloidal gelation. At low densities but for strong short-ranged attractions, particles are tightly bound to (asymptotically infinite) clusters and large elastic moduli result [18,19]. In this limit, the MCT equations can be simplified to one-parameter models which capture a number of the pertinent physical mechanisms although this neglects other aspects of the colloidal gels obtained which are connected to their self-similar structure on mesoscopic length scales.

In the following, the asymptotic models connected to colloidal gelation will be discussed further, where, especially, the existence of a divergent cluster size and its related dynamics is of interest. The strength of the required attractions at gelation is estimated also. Additionally, two unphysical aspects of the previously obtained MCT results for attractive Yukawa potentials and for Baxter's adhesive hard-sphere model (AHS) [18,22] are reconsidered using the controlled low-density virial expansion [23]. Adopting a very common model in colloid science, hard spheres interacting with a square-well potential are studied [24].

2. Basic equations

The simplest MCT equations for the normalized time-dependent intermediate-scattering functions at wave vector q, $\Phi_q(t)$, will be studied, as appropriate for the description of the structural relaxation of colloidal suspensions (characterized by a Brownian short-time diffusion coefficient D_q^s) [20,21,25]:

$$\partial_t \Phi_q(t) + q^2 D_q^s \left\{ \Phi_q(t) + \int_0^t \mathrm{d}t'\, m_q(t-t')\, \partial_{t'} \Phi_q(t') \right\} = 0. \tag{1}$$

Here, the generalized longitudinal viscosity is given by a mode coupling functional, $m_q(t) = \mathcal{F}_q([c], [\Phi(t)])$, which is uniquely specified by the equilibrium static structure as given by the direct correlation function c_q:

$$\mathcal{F}_q([c], [f]) = \frac{\rho S_q}{2q^4} \int \frac{\mathrm{d}\boldsymbol{k}\, \mathrm{d}\boldsymbol{p}}{(2\pi)^3}\, \delta(\boldsymbol{k}+\boldsymbol{p}=\boldsymbol{q})(\boldsymbol{q}\cdot\boldsymbol{p}c_p + \boldsymbol{q}\cdot\boldsymbol{k}c_k)^2 S_k S_p f_k f_p. \tag{2}$$

where ρ is the particle number density and c_q determines the static structure factor via $S_q = 1/(1-\rho c_q)$.

Non-ergodicity transitions of MCT dynamical equations are obtained as bifurcation points of the non-linear equations for the q-dependent non-ergodicity or Edwards–Anderson parameters f_q, which, in the idealized MCT, are defined as $\Phi_q(t \to \infty) = f_q$:

$$\frac{f_q}{1-f_q} = \mathcal{F}_q([c], [f]). \tag{3}$$

Whereas vanishing non-ergodicity parameters, $f_q = 0$, indicate fluid or ergodic states, finite ones, $f_q \geqslant f_q^c > 0$, spring into existence at larger interactions and signal the arrest of density fluctuations into non-equilibrium states, which are amorphous solids like gels or glasses. The idealized MCT assumes a separation of timescales describing the arrested structures as truly non-ergodic states, although further slow transport processes may lead to a decay of the arrested structures at much longer times; see the reviews [20,21] for discussions and extended theoretical approaches.

Whereas glass transitions have been studied extensively and are present in the colloidal suspensions studied at higher packing fractions also [4], non-ergodicity transitions into gel

states exhibit novel phenomena and anomalies connected to the low packing fractions and the resulting tenuous ramified gel structures. The experimentally observed small-angle scattering peaks indicating domain formation after quenches into states far from equilibrium are one aspect, which however is neglected here, because short local length scales are considered where local equilibrium may be assumed. Another aspect, the existence and growth of tightly bonded clusters, is signalled by the local dynamics; see below.

3. Virial expansion input

Specifying the static input, i.e. c_q, the bifurcation lines and the resulting long-time dynamics can be determined as functions of the thermodynamic control parameters, namely packing fraction, ϕ, and temperature, T. For colloidal particles characterized by steric repulsion and short-ranged attraction, the square-well potential is widely used [24]:

$$u(r) = \begin{cases} \infty & 0 < r < \sigma \\ -U_0 & \sigma < r \leqslant \sigma + \Delta \\ 0 & \sigma + \Delta < r. \end{cases} \tag{4}$$

The virial expansion provides a controlled approximation for dilute systems and determines the direct correlation function for low packing fractions as: $c(r) = f(r) + \mathcal{O}(\phi)$, where $f = \mathrm{e}^{-u(r)/k_BT} - 1$ is the Mayr cluster function [23]. The gel transitions can be studied in an asymptotic model of vanishing packing fraction and temperature, which describes a dilute system of strongly interacting particles [18, 19]. Within the virial expansion this limit is obtained for:

$$\phi \to 0 \text{ and } A \to \infty \qquad \text{so } \Gamma_v = \frac{12\Delta\phi A^2}{\pi^2\sigma} = \text{constant} \tag{5}$$

where $A = \mathrm{e}^{U_0/k_BT} - 1$. Note that this results in $S_q = 1$, because $\phi \to 0$, indicating that structural correlations can be neglected in explaining the gel non-ergodicity transitions. Thus, in this limit, glassy dynamics, due to caging at higher packing fractions, is absent as well as dynamics connected to critical phenomena, where long-ranged correlations are important; note that an increase in the compressibility (or $S_{q=0}$) would require lower temperatures than are considered in equation (5) as the virial estimate indicates: $S_{q\to 0} \to \infty$ for $\phi A\Delta/\sigma = 1/24 + \mathcal{O}(\phi, \Delta/\sigma)$. Moreover, as expected on physical grounds, only attractive potentials can lead to the limit equation (5) and thus to gels, because A would remain bounded for pure repulsions; this is violated by the mean-spherical approximation used in [18, 19].

4. Results for the gel structures

The results for the gel form factors f_q are of immediate interest as they provide information on the spatial correlations of the arrested solid-like structures.

In the specified limit of a strongly interacting dilute colloidal fluid, the mode coupling functional simplifies to a two-parameter model as its density and temperature dependence enters via Γ_v from equation (5) only: $\mathcal{F}_q([c], [f]) \to \mathcal{F}_q(\Gamma_v, \Delta/\sigma, [f])$. Figure 1 shows non-ergodicity parameters at the transition points for different well sizes, $\frac{1}{4} \leqslant \Delta/\sigma \leqslant 1$, and in the limit $\Delta \to 0$. At the gel transitions for $\Delta/\sigma \leqslant 0.76\ldots$, bonds of a length given by the attraction range are formed between the particles; the well size Δ sets the length scale for f_q^c. Above this width, the system arrests into somewhat different structures. In the non-ergodic states, fast particle rearrangements are possible on shorter distances, causing the decay of $\Phi_q(t = 0) = 1$ down to f_q, but small-wave-vector fluctuations are progressively suppressed

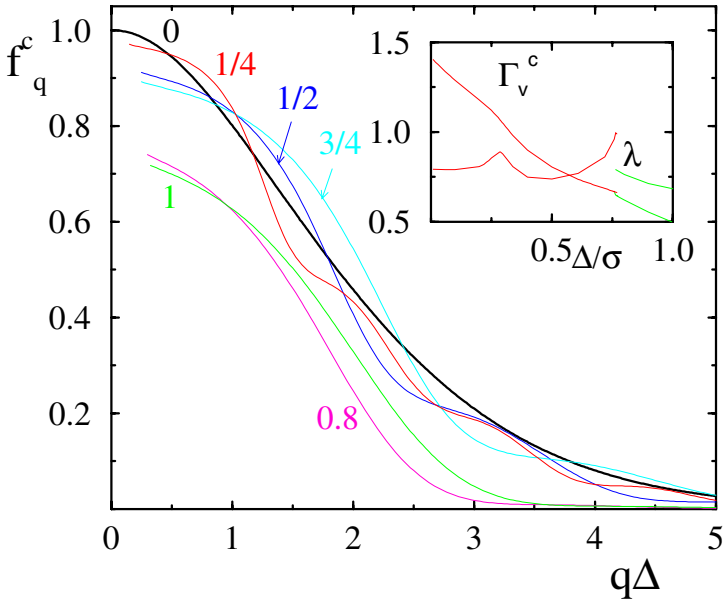

Figure 1. The critical non-ergodicity parameter f_q^c of strongly interacting dilute fluids described by equation (5) for the well sizes $\Delta/\sigma = \frac{1}{4}, \frac{1}{2}, \frac{3}{4}, 0.8, 1$ and in the limit $\Delta \to 0$; most curves are not shown below $q\Delta = 0.3$ because of numerical inaccuracies. The inset shows the variation of the critical coupling parameter Γ_v^c and of the exponent parameter λ with well size Δ.

upon decreasing Δ. Only for bond lengths or well sizes $\Delta \geqslant 0.2$ do appreciable large-distance temporal fluctuations of the gel structure exist.

The additional limit $\Delta/\sigma \ll 1$ is of interest, because the asymptotic model defined by equation (5) simplifies further and the results from figure 1 indicate that this limit qualitatively captures the gel structures (i.e. f_q^c) for Δ below $\approx$0.2. Moreover, the elastic constants of the gel increase strongly in this limit of short-ranged attractions, and thus observation of the non-ergodic gel states is more likely, as will be argued below.

A naive application of $\Delta \to 0$ leads to the AHS virial result: $c_q \to 4\pi A \Delta\sigma (\sin q\sigma)/q$. Because of its slow algebraic decay for $q \to \infty$, the wave-vector integration in equation (2) does not converge and the results depend on the chosen wave-vector cut-off $k_{\max}$. In the AHS model this holds for all temperatures and packing fractions as argued in [18]. However, first substituting the direct correlation function into equation (2), and then performing the limit $\Delta \to 0$ leads to a different and almost everywhere convergent memory kernel:

$$\mathcal{F}_{\tilde{q}}(\Gamma_v, [f]) = \frac{\Gamma_v}{\tilde{q}^2} \int \mathrm{d}^3\tilde{k} \left(\frac{\tilde{\boldsymbol{q}} \cdot \tilde{\boldsymbol{k}}}{\tilde{q}\tilde{k}^2} \right)^2 (1 - \cos\tilde{k}) f_{\tilde{k}} f_{|\tilde{\boldsymbol{q}} - \tilde{\boldsymbol{k}}|} \tag{6}$$

where $\tilde{q} = q\Delta$ denotes the rescaled wave vector. Tight localization of the particles is predicted by the solutions to equations (3) and (6) shown in figure 2, because the q-width of the Edwards–Anderson parameters f_q is given by the inverse of the narrow well width Δ. Binding to (in this limit) infinite clusters is described because the wave-vector-dependent longitudinal modulus diverges like $1/\tilde{q}^2$, even though it is connected to the total force acting among all particles, $q^2\mathcal{F}_q \propto \langle F_{\mathrm{tot}}^*(t \to \infty) F_{\mathrm{tot}}(0) \rangle$ for $q \to 0$, where the total force among all particles vanishes according to Newton's action–reaction principle, $F_{\mathrm{tot}} = 0$. In the specified limit, however, the particles experience forces from infinitely removed particles belonging to the same cluster,

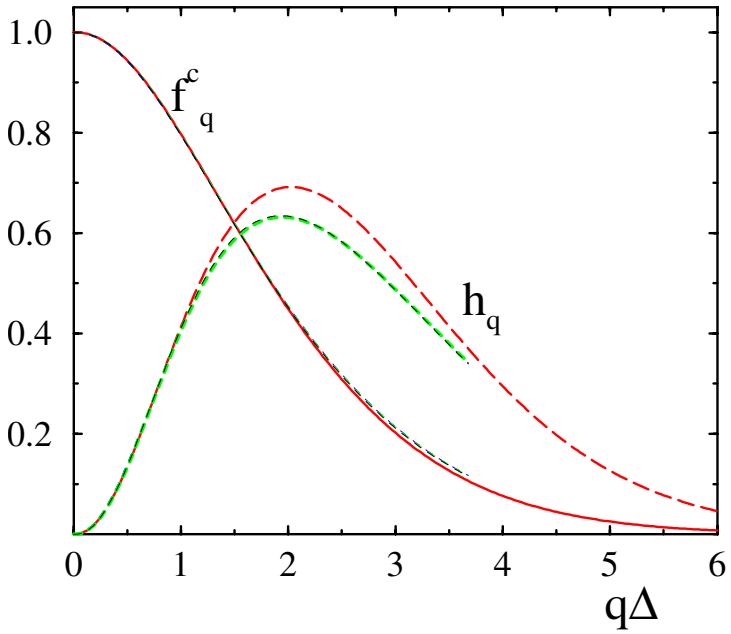

Figure 2. The non-ergodicity parameter f_q^c (full line) and critical amplitude h_q (long-dashed line) at the critical point of the virial model for the square-well potential. The thin short-dashed lines show the corresponding results from the AHS model obtained using the wave-vector cut-offs $k_{\max}\sigma = 40$, 80, and 160; the effective width is found as $\Delta_{\rm eff}^{\rm AHS} = 3.68/k_{\max}$.

and thus $q^2\mathcal{F}_q$ stays finite as the true $F_{\rm tot}$ cannot be determined. Collective and single-particle density fluctuations consequently become identical, $\Phi_q(t) = \Phi_q^s(t)$, leading e.g. to the limit $f_{\tilde{q}} \to 1 - (\tilde{q}\tilde{r}_s)^2$ for $\tilde{q} \to 0$, where the particle root mean square displacement, r_s, approaches (half) the well width, $\tilde{r}_s^c = r_s^c/\Delta = 0.48$, at the transition point; see also [18, 19].

Figure 2 shows the solution of equations (3) and (6) (evaluated, as in figure 1, with 400 grid points spaced at $\delta\tilde{q} = 0.025$) at the critical point $\Gamma_v^c = 1.42\ldots$, which corresponds to rather modest attractions; e.g. for $\Delta/\sigma = 1/100$ and $\phi = 0.1$ one finds $U_0/k_BT = 3.56$. Solutions from the AHS virial approximation are also included for three different cut-offs $k_{\max}\sigma = 40$, 80, and 160. One notices that for small wave vectors the solutions can be scaled onto the square-well result; also the AHS critical coupling parameter scales as one would expect: $\Gamma_v^{c\rm AHS} \propto 1/k_{\max}$. However, as all wave vectors for example enter the determination of the exponent parameter λ [20, 21, 26], appreciable differences result: $\lambda_v^{\rm AHS} = 0.65$ compared to $\lambda_v^{\rm Sq.W} = 0.79$.

5. Results for the dynamics

The bifurcations to non-ergodic solid-like states in equations (3) and (6) also lead to anomalies in the long-time dynamics which provide the most detailed information about the gel formation and the connected transport mechanisms. We focus on the limit of narrow attractions, $\Delta \ll \sigma$, as clustering is specific to the low-density transitions considered, and it is thus of interest to study the consequences of the small-q divergence of the longitudinal modulus.

In the limit given by equation (5) and for $\Delta \ll \sigma$, introduction of a rescaled time, $\tilde{t} = tD_0/\Delta^2$ with $D_0 = D_{q\to\infty}^s$, eliminates the transient parameters and leads to simplified

equations of motion for the coherent (and identically for the incoherent) density fluctuations:

$$\partial_{\tilde{t}}\Phi_{\tilde{q}}(\tilde{t}\,) + \tilde{q}^2\Phi_{\tilde{q}}(\tilde{t}\,) + \int_0^{\tilde{t}} \mathrm{d}\tilde{t}'\; \tilde{m}_{\tilde{q}}(\tilde{t}-\tilde{t}')\,\partial_{\tilde{t}'}\Phi_{\tilde{q}}(\tilde{t}') = 0 \tag{7}$$

where the friction function is given by $\tilde{m}_{\tilde{q}}(\tilde{t}\,) = \tilde{q}^2\mathcal{F}_{\tilde{q}}(\Gamma_v, [\Phi])$, and the initial variation is $\Phi_{\tilde{q}}(t) = 1 - \tilde{q}^2\tilde{t} + \cdots$.

Figure 3 shows intermediate-scattering functions for a range of interaction parameters and wave vectors. The two-step relaxation can be analysed with the techniques developed for MCT glass transitions [20, 21]. It exhibits the factorization property during an intermediate time window: $\Phi_{\tilde{q}}(\tilde{t}\,) = f^c_{\tilde{q}} + h_{\tilde{q}}G^\lambda(\tilde{t}\,)$ for $|\Phi_{\tilde{q}} - f^c_{\tilde{q}}| \ll 1$, which enlarges upon approaching Γ^c_v. The β-correlator, G^λ, captures the sensitive dependences on time and interaction strength, and the amplitudes $f^c_{\tilde{q}}$ and $h_{\tilde{q}}$ (see figure 2) describe the gel structure and the spatial correlations of the mechanism dominating the bond formation. Power-law decays around the plateau value f^c and the divergence of a first scaling time are contained in $G^\lambda(\tilde{t}\,)$.

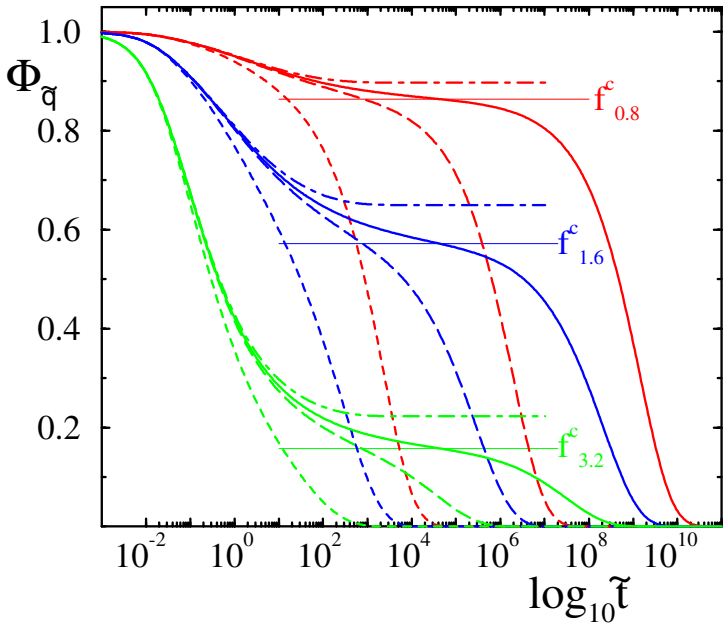

Figure 3. Intermediate-scattering functions $\Phi_{\tilde{q}}(\tilde{t}\,)$ determined from (7). For the interaction parameters $\Gamma_v/\,\Gamma^c_v = 0.9$, 0.99, 0.999, and 1.01, corresponding to the short-, long-dashed, solid and dashed–dotted curves, solutions for the wave vectors $\tilde{q} = 0.8$, 1.6, and 3.2 are shown. The thin horizontal lines indicate the critical non-ergodicity parameters $f^c_{\tilde{q}}$ which give the long-time limits, $f^c_{\tilde{q}} = \Phi_{\tilde{q}}(\tilde{t} \to \infty)$ at $\Gamma^c_v = 1.3647$ for the chosen discretization, $\delta\tilde{q} = 0.08$ and 100 grid points.

The near arrest of the $\Phi_{\tilde{q}}(\tilde{t}\,)$ around $f^c_{\tilde{q}}$ leads to an intermediate elastic behaviour of the gel, which in the limit studied follows from the asymptotic result for the shear modulus G:

$$G(\tilde{t}\,) = (k_BT\rho)\frac{\pi\Gamma_v\sigma^2}{20\Delta^2}\int_0^\infty \mathrm{d}\tilde{k}\;(1-\cos\tilde{k})\Phi^2_{\tilde{k}}(\tilde{t}\,). \tag{8}$$

Figure 4 shows the corresponding storage and loss moduli which, in the fluid, exhibit a near-elastic plateau with power-law corrections predicted by the β-correlator G^λ. Using the initial variation of $\Phi_{\tilde{q}}(\tilde{t}\,)$, a high-frequency divergence, $G'(\tilde{\omega}) \propto G''(\tilde{\omega}) \propto \tilde{\omega}^{1/2}$ for $\tilde{\omega} \to \infty$ results

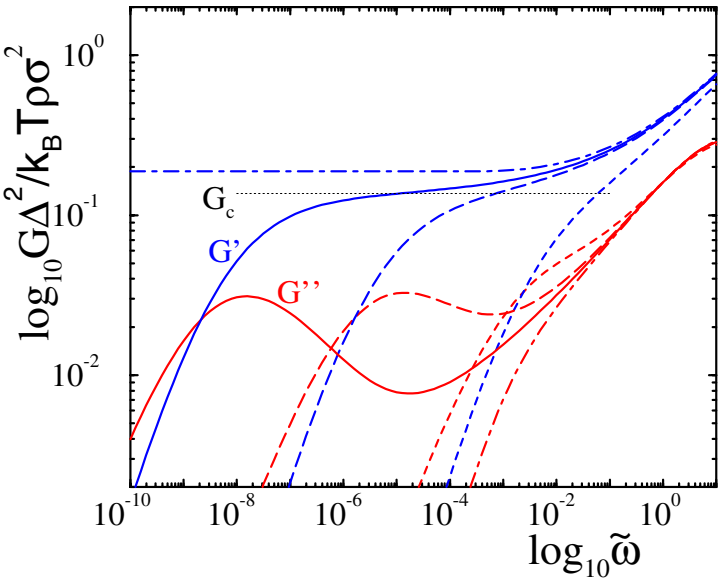

Figure 4. Storage, $G'(\tilde{\omega})$, and loss, $G''(\tilde{\omega})$, moduli according to equation (8) for the interaction parameters and line styles of figure 3. The horizontal line indicates the critical elastic modulus, G_c, of the gel at the transition, $\Gamma_v = \Gamma_v^c$.

from the integration in equation (8) at high k. This result, which is familiar for colloidal hard spheres in the absence of hydrodynamic interactions [24], cannot be seen in figure 4 because of the chosen small-wave-vector cut-off.

Importantly, equation (8) predicts that large, $\mathcal{O}((\sigma/\Delta)^2)$, elastic moduli result upon formation of the gels for $\Gamma \geqslant \Gamma_v^c$, if the particles interact via short-ranged attractions†. The elastic modulus at the transition, G_c, which follows from equation (8) and from the critical gel structure factors, $f_{\tilde{q}}^c$, is included in figure 4.

The final decay of the intermediate-scattering functions or of the shear modulus G is described asymptotically by the second MCT scaling law, which entails the existence of a second set of divergent timescales and of Γ_v-independent and non-exponential relaxation functions [20, 21]. The small-q divergence of the longitudinal modulus leads to a diffusive behaviour of the final relaxation times, $\tilde{\tau}_{\tilde{q}} \propto \tilde{\tau}_{\tilde{q}}^{\infty}(\Gamma_v^c - \Gamma_v)^{-\gamma}$, with Γ_v-independent amplitude $\tilde{\tau}_{\tilde{q}}^{\infty} \propto 1/\tilde{q}^2$. Here the exponent γ is determined by λ, and follows as $\gamma = 2.85$. The diffusive behaviour is apparent in figure 3 and emphasizes that the final melting of the precursor gel structure in the fluid phase requires transport over large distances which scale like σ/Δ^2 as follows from equation (6). Again this indicates the presence of infinite clusters which arrest and cannot melt any longer at and above the gel transition at Γ_v^c.

6. Conclusions

We have provided further support for the suggestion that colloidal gelation is caused by non-ergodicity transitions triggered on local distances [18, 19].

It was shown that non-ergodic structures characterized by strong elastic moduli are obtained in dilute solutions of colloidal particles interacting with short-ranged attractions

† Note an error in [18] where G corrected to $G \propto K_c^2\phi_c^2/b^3$ shows the same scaling behaviour as the present result.

upon lowering the temperature. Bonds with a length given by the attraction range are formed between the particles if the strength of the attraction increases to a few $k_B T$. These values are in qualitative agreement with phenomenological considerations for reversible gelation [3, 10]. We suggest that this formation of long-lived bonds is the rate-limiting step for (transient) gelation in colloidal suspensions.

The formation of (percolated) clusters is indicated by the long-ranged force correlations of the arrested structures which cause the small-wave-vector divergence of the mode coupling functional $\mathcal{F}_q$. The description of the mesoscopic gel structure and of the related domain-coarsening kinetics, however, has not yet been incorporated into the present approach.

The long-ranged force correlations at the gel non-ergodicity transitions cause the collective and single-particle dynamics to become identical for long times, and lead to the one mode coupling functional determining all time-dependent small-wave-vector quantities, like the mean square displacement or moduli; such connections have already been exploited to measure the elastic response via light scattering techniques [27]. Moreover, a diffusive final relaxation of the colloid density fluctuations results close to the gel transitions, $\tau_q \propto 1/q^2$, which suggests that a generalized Gaussian description, $\Phi_q(t) = \exp\{-(q^2/6)\,\delta r^2(t)\}$, as suggested by Segrè and Pusey [28], can provide a reasonable description of the long-time dynamics for all wave vectors; note that for colloidal suspensions at the glass transition this *ansatz* failed at small wave vectors because of the non-diffusive structural relaxation [28, 29].

Using the exact low-density virial expansion, two at first sight unphysical aspects of previous MCT calculations were identified as artefacts of the approximate static structural input. First, the cut-off dependence found within the AHS model [18, 22] was analysed for low densities. The interesting conclusion is that MCT predicts the AHS model to be in the non-ergodic state for any non-zero particle concentration. Second, it was clarified that gelation requires attractive interactions.

Dynamic light scattering measurements as performed by van Megen and co-workers at the colloidal glass transition [30–32] or further viscoelastic measurements [7, 27] can provide crucial tests of our approach. First measurements of the non-ergodicity parameters support it [33]. Dynamic light scattering measurements of Krall and Weitz [34] also show intriguing connections and require further study.

Acknowledgments

Valuable discussions with Dr P N Segrè, Professor D A Weitz, Professor M E Cates, and Professor W Götze are gratefully acknowledged. MF was supported by the Deutsche Forschungsgemeinschaft under Grant No Fu 309/3.

References

[1] Carpinetti M and Giglio M 1992 *Phys. Rev. Lett.* **68** 3327
[2] Bibette J, Mason T G, Gang H and Weitz D A 1992 *Phys. Rev. Lett.* **69** 981
[3] Poon W C K and Haw M D 1997 *Adv. Colloid Interface Sci.* **73** 71
[4] Poon W C K, Selfe J S, Robertson M B, Ilett S M, Pirie A D and Pusey P N 1992 *J. Physique* II **3** 1075
[5] Poon W C K, Pirie A D and Pusey P N 1995 *Faraday Discuss.* **101** 65
[6] Grant M C and Russel W B 1993 *Phys. Rev.* E **47** 2606
[7] Rueb C J and Zukoski C F 1998 *J. Rheol.* **42** 1255
[8] Poulin P, Bibette J and Weitz D A 1999 *Eur. Phys. J.* B **7** 277
[9] Verduin H and Dhont J K G 1995 *J. Colloid Interface Sci.* **172** 425
[10] Verhaegh N A M, Asnaghi D, Lekkerkerker H N W, Giglio M and Cipelletti L 1997 *Physica* **242** 104
[11] Muschol M and Rosenberger F 1997 *J. Chem. Phys.* **107** 1953

[12] ten Wolde P R and Frenkel D 1997 *Science* **277** 1975
[13] Rosenbaum D, Zamora P C and Zukoski C F 1996 *Phys. Rev. Lett.* **76** 150
[14] Poon W C K 1997 *Phys. Rev.* E **55** 3762
[15] Evans R M L, Poon W C K and Cates M E 1997 *Europhys. Lett.* **38** 595
[16] Bray A J 1994 *Adv. Phys.* **43** 357
[17] Sciortino F and Tartaglia P 1995 *Phys. Rev. Lett.* **74** 282
[18] Bergenholtz J and Fuchs M 1999 *Phys. Rev.* E **59** 5706
[19] Bergenholtz J and Fuchs M 1999 *J. Phys.: Condens. Matter* **11** 10 171
[20] Götze W 1991 *Liquids, Freezing and Glass Transition* ed J-P Hansen, D Levesque and J Zinn-Justin (Amsterdam: North-Holland) p 287
[21] Götze W and Sjögren L 1992 *Rep. Prog. Phys.* **55** 241
[22] Fabbian L, Götze W, Sciortino F and Thiery P T F 1999 *Phys. Rev.* E **59** R1347
[23] Hansen J-P and McDonald I R 1986 *Theory of Simple Liquids* (London: Academic)
[24] Russel W B, Saville D A and Schowalter W R 1989 *Colloidal Dispersions* (New York: Cambridge University Press)
[25] Bengtzelius U, Götze W and Sjölander A 1984 *J. Phys. C: Solid State Phys.* **17** 5915
[26] Götze W 1985 *Z. Phys.* B **60** 195
[27] Mason T G and Weitz D A 1995 *Phys. Rev. Lett.* **75** 2770
[28] Segrè P N and Pusey P N 1996 *Phys. Rev. Lett.* **77** 771
[29] Fuchs M and Mayr M R 1999 *Phys. Rev.* E **60** 5742
[30] van Megen W and Underwood S M 1993 *Phys. Rev. Lett.* **70** 2766
[31] van Megen W and Underwood S M 1994 *Phys. Rev.* E **49** 4206
[32] van Megen W, Mortensen T C, Müller J and Williams S R 1998 *Phys. Rev.* E **58** 6073
[33] Poon W C K, Starrs L, Meeker S P, Moussaïd A, Evans R M, Pusey P N and Soliva M F 1999 *Faraday Discuss.* **112** 143
[34] Krall A H and Weitz D A 1998 *Phys. Rev. Lett.* **80** 778